

Self-consistent treatment of the self-energy in nuclear matter

Kh. Gad* and E.M. Darwish

Physics Department, Faculty of Science, South Valley University, Sohag, Egypt

Abstract

The influence of hole-hole propagation in addition to the conventional particle-particle propagation, on the energy per nucleon and the momentum distribution is investigated. The results are compared to the Brueckner-Hartree-Fock (BHF) calculations with a continuous choice and conventional choice for the single-particle spectrum. The Bethe-Goldstone equation has been solved using realistic NN interactions. Also, the structure of nucleon self-energy in nuclear matter is evaluated. All the self-energies are calculated self-consistently. Starting from the BHF approximation without the usual angle-average approximation, the effects of hole-hole contributions and a self-consistent treatment within the framework of the Green function approach are investigated. Using the self-consistent self-energy, the hole and particle self-consistent spectral functions including the particle-particle and hole-hole ladder contributions in nuclear matter are calculated using realistic NN interactions. We found that, the difference in binding energy between both results, i.e. BHF and self-consistent Green function, is not large. This explains why is the BHF ignored the 2h1p contribution.

Key words:

Nuclear matter, Green function, Spectral function, Binding energy.

1 Introduction

It is one of the fundamental issue in nuclear physics to evaluate the nuclear matter binding energy and saturation properties, starting from a realistic nucleon-nucleon (NN) interaction without any adjustment of a free parameter [1,2,3]. The solution of this problem is of great interest, because the understanding of the binding energy of nuclei is one of the basic problems of nuclear

* e-mail: kha92@yahoo.com

physics and physics in general. Because of the presence of strongly repulsive components in the short-range part of the NN interaction [4,5,6], the NN scattering correlation has a predominant importance in the nuclear matter calculation. The solution of this problem is also very important because the nuclear many-body problem is one of the most challenging testing grounds for many-body theories of quantum systems. Last not least, however, a microscopic understanding of the binding energy of normal nuclei, which is based on a realistic model for the NN interaction, shall also provide a reliable prediction for the equation of state of nuclear matter at densities beyond the saturation density of normal nuclei, which is required for the study of astrophysical objects like the explosion of supernova and the structure of neutron stars.

Recently, Various approximation schemes have been developed to describe the correlations which are induced into the many-nucleon wave function by the strong short-range and tensor components of such a realistic NN force. For a recent review on such methods see, e.g., Refs. [7,8]. The resulting correlation functions are the key input for the study of the absorption of real and virtual photons by pairs of nucleons as it is observed in (γ, NN) or $(e, e' NN)$ reactions. One of the most popular approximation schemes, which is frequently used in nuclear physics, is the Brueckner-Bethe-Goldstone (BBG) theory [1] which has been one of the tools for solving the many-body problem of nuclear matter for many years [8,9,10,11]. The results of BHF calculations depend on the choice of the single particle potential, $U(k)$. In the conventional choice, $U = 0$ for $k > k_F$, and U is the self-consistent BHF potential for $k < k_F$. The alternative "continuous" choice has been proposed in [12] for which U is again the self-consistent BHF potential, but it extends to $k > k_F$. This continuous choice leads to an enhancement of correlation effects in the medium and tends to predict larger binding energies for nuclear matter than the conventional choice.

In this paper, special attention will be paid to study the self-consistent self-energy. Note, that all the self-energies in this paper will be calculated self-consistently. The self-energy of a nucleon contains all the information necessary to obtain occupation probabilities, quasi-particle strength and broadening features which alternatively can be visualized in terms of hole and particle spectral functions.

It is the purpose of this paper to investigate whether an improved and more consistent treatment of the many-body system, still based on nonrelativistic dynamics and two-body forces, can provide new information on the saturation problem of nuclear matter. A self-consistent treatment of the Green's functions formalism leads to the so called self-consistent Green's function (SCGF) theory [13,14,15,16,17,18,19]. Attempts have been made to employ the technique of a self-consistent evaluation of Green's functions [20,21] to the solution of

the nuclear many-body problem. This method offers various advantages: (i) The single-particle Green's function contains detailed information about the spectral function, i.e. the distribution of single-particle strength, to be observed in nucleon knock-out experiments, as a function of missing energy and momentum. (ii) The method can be extended to finite temperatures [5,22], a feature which is of interest for the study of the nuclear properties in astrophysical environments. (iii) The BHF approximation, the approximation to the hole-line expansion which is commonly used, can be considered as a specific approximation within this scheme. Attempts have been made to start from the BHF approximation and include the effects of the hole-hole scattering terms in a perturbative way [23,24]. There is a good reason to believe that a more complete treatment of the nucleon self-energy in the full framework of Green-function theory will ultimately help resolve long standing questions about nuclear saturation. Via this study we will be able to give an answer to a fundamental question regarding reliability of the BHF theory. Application of SCGF theory has proven useful for understanding the location and quantity of single-particle strength found in the electron-scattering experiments. The focus of this paper is to apply SCGF theory to nuclear matter to study the nucleon properties.

After this introduction we will discuss some features of the self-consistent BHF approach for the self-consistent self-energy in Sec. 2. The effect of the hole-hole terms in the self-consistent self-energy and a self-consistent Green-function will be presented in Sec. 3. The self-consistent spectral function will be presented in Sec. 4. The main conclusions are summarized in the final section.

2 BHF approximation

One of the central equations to be solved in the BHF approximation is the Bethe-Goldstone equation. It is given by

$$\begin{aligned} \langle k'_1 k'_2 | G(\omega) | k_1 k_2 \rangle = & \langle k'_1 k'_2 | v | k_1 k_2 \rangle + \sum_{k_3 k_4} \langle k'_1 k'_2 | v | k_3 k_4 \rangle \\ & \times \frac{Q(k_3, k_4)}{\omega - E(k_3, k_4)} \langle k_3 k_4 | G(\omega) | k_1 k_2 \rangle, \end{aligned} \quad (1)$$

where v is the bare potential, ω denotes the starting energy, Q is the Pauli operator which requires the nucleon momenta to be outside the Fermi sea, E is the sum of the two single-particle energies inside nuclear matter given by

$$E(k_1, k_2) = \varepsilon_{k_1} + \varepsilon_{k_2}, \quad (2)$$

with the single particle energies

$$\varepsilon_k = \frac{k^2}{2m} + \text{Re} \Sigma^{BHF}(\vec{k}, \omega = \varepsilon_k), \quad (3)$$

where the self-energy of a nucleon in nuclear matter with momentum \vec{k} is determined by the self-consistent equation

$$\Sigma^{BHF}(\vec{k}, \omega) = \int d^3k' \langle \vec{k}\vec{k}' | G(\varepsilon_k + \varepsilon_{k'}) | \vec{k}\vec{k}' \rangle n_0(\vec{k}'), \quad (4)$$

with the occupation probability of a free Fermi gas with a Fermi momentum k_F

$$n_0(\vec{k}') = \begin{cases} 1 & \text{for } |\vec{k}'| \leq k_F \\ 0 & \text{for } |\vec{k}'| > k_F \end{cases}. \quad (5)$$

In the BHF approximation, (1), (3), and (4) are solved self-consistently.

The definition of the single-particle potential or the self-energy can be extended beyond the BHF approximation. In order to discuss such an extension we want to consider various contributions, which are represented by the diagrams or series of diagrams displayed in Fig. 1. These terms are summed up in a self-energy as can be written schematically by

$$\begin{aligned} \Sigma(k, \omega) &= \Sigma^{HF}(k) + \Delta\Sigma^{2p1h}(k, \omega) + \Delta\Sigma^{2h1p}(k, \omega) \\ &= \Sigma^{BHF}(k, \omega) + \Delta\Sigma^{2h1p}(k, \omega), \end{aligned} \quad (6)$$

where the contribution due to two-particle one-hole terms $\Delta\Sigma^{2p1h}$ is complex for $\omega > \varepsilon_F$ while the two-hole one-particle term $\Delta\Sigma^{2h1p}$ is complex for $\omega < \varepsilon_F$. The imaginary part of the BHF self-energy vanishes for $\omega < \varepsilon_F$.

Real and imaginary parts of the self-energy are related to each other by a dispersion relation of the form [25,26]

$$\text{Re}\Sigma^{BHF}(k, \omega) = \Sigma^{HF}(k) + \frac{1}{\pi} \int_{-\infty}^{\infty} \frac{\text{Im} \Sigma^{BHF}(k, \omega')}{\omega' - \omega} d\omega'. \quad (7)$$

$$\text{Re}\Delta\Sigma^{2h1p}(k, \omega) = \frac{1}{\pi} \int_{-\infty}^{\infty} \frac{\text{Im} \Delta\Sigma^{2h1p}(k, \omega')}{\omega' - \omega} d\omega', \quad (8)$$

The self-energy of the Hartree-Fock term is real and independent of ω . It is given as [27]

$$\Sigma^{HF}(k) = \sum_{k'} \langle kk' | V | kk' \rangle n(k'), \quad (9)$$

where $n(k')$ is the single particle occupation probability. The importance of the Hartree-Fock term is that it represents the simplest solution to the many body problem.

The energy dependence of the real part of the BHF self-consistent self-energy (see (4)) is visualized in Figs. 2 and 3, for nuclear matter with Fermi momentum $k_F = 1.36 \text{ fm}^{-1}$. It is evaluated for the CD-Bonn [28] and Bonn C potential [29], for various momenta k . This real part displays a pronounced minimum at energies around the Fermi energy. These results have been obtained after establishing self-consistency for the single-particle spectrum according to (3)

Figs. 4 and 5 show the imaginary part of the BHF self-consistent self-energy as a function of ω evaluated for the CD-Bonn (Fig. 4) and Bonn C (Fig. 5) potentials, respectively, for different values of momenta k . We see that the imaginary part is identical zero for energies ω less than $\varepsilon_k - \varepsilon_F$, as can be seen from (3), and yield non-negligible values up to very high energies. Although not explicitly shown in Figs. 4 and 5, $\text{Im}\Sigma^{BHF}(k, \omega)$ vanishes at high energies which is a consequence of the vanishing of the imaginary G matrix elements at very large values of the energy parameter. This result is general for any soft-core interaction, although the softness of the core directly influences the energy for which the matrix elements become negligible. Considering the results for the imaginary part of the self-consistent self-energy, which are displayed in Figs. 4 and 5, it is clear from the dispersion relation (7) that the real part of the self-energy is identical to the corresponding HF single-particle potential $\Sigma^{HF}(k)$ in the limit $\omega \rightarrow -\infty$. This real part gets more attractive with increasing ω until one reaches values of ω at which the imaginary part is different from zero. The self-energy turns less attractive at higher energies, which leads to a pronounced minimum at energies ω slightly above the Fermi energy.

The conventional choice has been to ignore self-energy contributions for the particle states completely and approximate the energies by the kinetic energy only. This conventional choice for the single-particle spectrum, however, is not very appealing as it leads to a gap at the Fermi surface: the propagator for single-particle states with momenta below the Fermi momentum k_F is described in terms of a bound single-particle energy while the corresponding spectrum for the particle states starts at the kinetic energy for the momentum k_F , so the potential in this case is given by [30]

$$U(k) = \begin{cases} \sum_{k' \leq k_F} \langle kk' | G(\omega = \varepsilon_k + \varepsilon_{k'}) | kk' \rangle_A: & k \leq k_F \\ 0 & k > k_F \end{cases} . \quad (10)$$

Alternatively, a continuous choice for the potential can be made [29] by defining

$$U(k) = \text{Re} \sum_{k' \leq k_F} \langle kk' | G(\omega = \varepsilon_k + \varepsilon_{k'}) | kk' \rangle_A , \quad (11)$$

for all states k below and above the Fermi surface. This leads to a spectrum that is continuous at the Fermi momentum. Where $|kk' \rangle_A = |kk' \rangle - |k'k \rangle$.

The self-consistent single-particle potential can be written as follows

$$U_{BHF}(k) = Re \sum^{BHF} (k, \omega = \varepsilon_k). \quad (12)$$

Fig. 6 displays the single-particle self-consistent potentials as a function of momentum at different densities using the CD-Bonn potential. The single-particle potential at $k_F=1.36 \text{ fm}^{-1}$ shows a significant deviation from a parabolic shape in particular at momenta slightly above the Fermi momentum, see also [31,32,33]. It is obvious that such a deviation tends to provide more attractive matrix elements of G in evaluating the self-energy for hole states according to (4), which leads to more binding energy. At high Fermi momentum ($k_F = 2.04 \text{ fm}^{-1}$ and $k_F = 2.72 \text{ fm}^{-1}$) this deviation is disappear.

3 Self-consistent Green functions

In the self-consistent Green's function (SCGF) formalisms, the self-energy is the key quantity to determine the one-body Green's function. One can calculate the contribution of the hole-hole terms to the self-energy in a kind of perturbative way [34]

$$\Delta\Sigma^{2h1p}(k, \omega) = \int_{k_F}^{\infty} d^3p \int_0^{k_F} d^3h_1 d^3h_2 \frac{\langle k, p | G | h_1, h_2 \rangle^2}{\omega + \tilde{\varepsilon}_p - \tilde{\varepsilon}_{h_1} - \tilde{\varepsilon}_{h_2} - i\eta}. \quad (13)$$

We assume a single-particle spectrum $\tilde{\varepsilon}_k$ which is identical to the self-consistent BHF spectrum, but shifted by a constant C_1 , which ensures the self-consistency for $k = k_F$

$$\begin{aligned} \tilde{\varepsilon}_{k_F} &= \varepsilon_{k_F}^{BHF} + C_1 \\ &= \frac{k_F^2}{2m} + Re [\Sigma^{BHF}(k_F, \omega = \tilde{\varepsilon}_{k_F}) + \Delta\Sigma^{2h1p}(k_F, \omega = \tilde{\varepsilon}_{k_F})]. \end{aligned} \quad (14)$$

This shifted single-particle spectrum is also used in the Bethe-Goldstone equation.

Results for the two-hole one-particle contribution to the self-consistent self-energy, $\Delta\Sigma^{2h1p}$, are displayed in Figs. 7 and 8, for various momenta k . Fig. 8 illustrates the self-consistent solutions of the imaginary part of the self-energy, including only 2h1p. The imaginary part of $\Delta\Sigma^{2h1p}$ is different from zero only for energies ω below the Fermi energy. This implies that $Im \Sigma^{2h1p}(k, \omega) = 0$, for $\omega = \varepsilon_F$. From (8) one also observes, noting that the imaginary part of $\Delta\Sigma^{2h1p}(k, \omega)$ is positive, that for $k = k_F$ the on-shell value of the real part

($\omega = \varepsilon_F$) must be positive. It turns out that this holds for all single particle momenta below k_F . The conservation of the total momentum in the two-nucleon of the G-matrix in (13), $\vec{h}_1 + \vec{h}_2 = \vec{k} + \vec{p}$, leads to a minimal value of ω at which this imaginary part is different from zero. Due to these limitations the imaginary part integrated over all energies is much smaller for $\Delta\Sigma^{2h1p}$ than for Σ^{BHF} . The real part of $\Delta\Sigma^{2h1p}$ is related to the imaginary part by a dispersion relation similar to the one of (8), connecting the imaginary part of Σ^{BHF} with the particle-particle ladder contributions to the real part of Σ^{BHF} . Since the imaginary part of $\Delta\Sigma^{2h1p}$ is significantly smaller than the one of Σ^{BHF} , the same is true also for the corresponding real part. The contribution of $\Delta\Sigma^{2h1p}(k, \omega)$ term is considerably smaller than the contribution of $\Sigma^{BHF}(k, \omega)$. At first sight this seems to confirm the notation that the effects of hh-propagation are considerably smaller than those corresponding to pp-propagation present in G-matrices.

The Lehmann representation of the Green's function for infinite nuclear matter is given by [35]

$$g(k, \omega) = \int_{-\infty}^{\varepsilon_F} d\omega' \frac{S_h(k, \omega')}{\omega - \omega' - i\eta} + \int_{\varepsilon_F}^{\infty} d\omega' \frac{S_p(k, \omega')}{\omega - \omega' + i\eta}, \quad (15)$$

where $S_{h(p)}(k, \omega)$ is the hole (particle) spectral function and we will discuss it in detail in the next section.

The formal solution of Dyson's equation is particularly simple in an infinite system,

$$g(k, \omega) = \frac{1}{\omega - \frac{k^2}{2m} - \Sigma(k, \omega)}. \quad (16)$$

In this approximation the solution of the Dyson equation leads only to a shift in the single particle energy according to (3). The Green's function expression for the binding energy is given by [36,31]

$$\frac{E}{A} = \frac{\int d^3k \int_{-\infty}^{\varepsilon_F} d\omega S_h(k, \omega) \frac{1}{2} \left(\frac{k^2}{2m} + \omega \right)}{\int d^3k n(k)}. \quad (17)$$

Results for the binding energy per nucleon are displayed in Table 1. In this table we have compared results for the binding energy of nuclear matter using the CD-Bonn potential from different prescriptions; (i) Hartree-Fock, (ii) BHF (using continuous choice), and (iii) BHF+2h1p (using conventional choice where the self-energy is calculated self consistently). The continuous choice leads to an enhancement of correlation effects in the medium and tends to predict larger binding energies for nuclear matter than the conventional choice. The conventional choice has been to ignore self-energy contribution for the particle states completely and approximate the energies by the kinetic energy only, see

(10). In nuclear matter one observes, that the inclusion of the 2h1p terms in the self-energy leads to less attractive quasiparticle energies, but more binding energy. The gain in binding energy due to the 2h1p components in the self-energy is about 0.5 MeV per nucleon in nuclear matter at saturation density [31]. We found that, no large difference in binding energy between both results, i.e. BHF and BHF+2h1p.

4 Self-consistent spectral function

The physical meaning of the spectral functions is rather simple. The hole spectral function $S_h(k, \omega)$ is the probability of removing a particle with momentum k from the target system of A particles leaving the resulting $(A - 1)$ system with an energy $E^{A-1} = E_0^A - \omega$, where E_0^A is the ground state energy of the target. Analogously, the particle spectral function $S_p(k, \omega)$ is the probability of adding a particle with momentum k and leaving the resulting $(A+1)$ system with an excitation energy ω measured with respect to the ground state of the A system, i.e., $\omega = E^{A+1} - E_0^A$. The spectral functions are obtained from the Dyson equation [25]. For the hole spectral function this yields the relation to the self-energy given by

$$\begin{aligned} S_h(k, \omega) &= \frac{1}{\pi} \text{Im} \, g(k, \omega) \\ &= \frac{1}{\pi} \frac{\text{Im} \, \Sigma(k, \omega)}{(\omega - k^2/2m - \text{Re}\Sigma(k, \omega))^2 + (\text{Im} \, \Sigma(k, \omega))^2}. \end{aligned} \quad (18)$$

The importance of the particle spectral function is to exhibit where the missing single-particle strength is located in energy. It is obtained by solving the Dyson equation and is related to the self-energy by

$$S_p(k, \omega) = -\frac{1}{\pi} \frac{\text{Im}\Sigma(k, \omega)}{(\omega - k^2/2m - \text{Re}\Sigma(k, \omega))^2 + (\text{Im}\Sigma(k, \omega))^2}. \quad (19)$$

In Figs. 9 and 10 a typical example of a hole spectral functions, for three different momenta in nuclear matter at $k_F = 1.36 \text{ fm}^{-1}$ as a function of energy. The self-consistent spectral function (SCSF) calculation is performed for the CD-Bonn and Bonn C potentials. The self-consistent particle spectral function displays a peak at ε_{qp} because of the vanishing term in the denominator of (18). Notice that as $k \rightarrow k_F$ this peak becomes extremely sharp due to the vanishing $\text{Im} \, \Sigma(k, \omega)$ in (18).

In Figs. 11 and 12 a typical example of a particle spectral functions, for three different momenta in nuclear matter at $k_F = 1.36 \text{ fm}^{-1}$ as a function of energy.

The SCSF calculation is performed for the CD-Bonn and Bonn C potentials. For momenta larger than k_F a quasi-particle peak, which, as usual, broadens with increasing momentum, can be observed on top of the same high energy tail. The results therefore display a common, essentially momentum independent, high-energy tail. The location of single particle strength at high energy simply means that the interaction has sufficiently large matrix elements.

The quasi-particle contribution can be isolated from the exact single particle propagator for k close to k_F by expanding the self-energy around the Fermi energy and employing the fact that the imaginary part of the self-energy behaves like $(\omega - \varepsilon_F)^2$ [37]. The quasi-particle energy is given by

$$\varepsilon_{SCGF}^{qp}(k) = \frac{k^2}{2m} + \text{Re}\Sigma(k, \varepsilon_{SCGF}^{qp}(k)), \quad (20)$$

which coincides with (3). With these ingredients one obtains in the limit $k \rightarrow k_F$ a δ -function contribution to the single particle propagator. Since the imaginary part is typically small around ε_F , this quasi-particle behavior is also obtained for other momenta close to k_F .

Fig. 13 displays the single-particle energy $\varepsilon(k)$ (see (10) and (11)) as a function of the momentum, at $k_F=1.2 \text{ fm}^{-1}$ using CD-Bonn potential. In this figure we displayed the single particle energies for continuous choice, single particle energies below k_F for SCGF using the conventional choice and the quasi particle energy (20). To obtain correct sum rules for momenta close to the Fermi momentum k_F , the quasi-particle approximation is used to isolate this part of the propagator explicitly. The quasi-particle strength $z(k)$ is given as [12]

$$z(k) = \left[1 - \left(\frac{\partial \text{Re}\Sigma(k, \omega)}{\partial \omega} \right)_{\omega=\varepsilon_{qp}(k)} \right]^{-1}, \quad (21)$$

where the quasi-particle strength in nuclear matter at $k_F = 1.36 \text{ fm}^{-1}$ using various models for the NN interaction are shown in Fig. 14. For comparison, results from the full many-body calculation (at $k_F = 1.33 \text{ fm}^{-1}$) of Benhar *et al.* [38] (dots) are also shown in Fig. 14.

Integrating the hole spectral function $S_h(k, \omega)$ over all the accessible excited states of the (A-1) system, one obtains the occupation probability of the single particle momentum k in the correlated ground state. The single nucleon momentum distribution in nuclear matter is defined as

$$n(k) = \int_{-\infty}^{\varepsilon_F} S_h(k, \omega) d\omega = 1 - \int_{\infty}^{\varepsilon_F} S_P(k, \omega) d\omega. \quad (22)$$

The momentum distribution is calculated self-consistent. Results are displayed in Fig. 15 for the CD-Bonn and Bonn C potentials at $k_F = 1.36 \text{ fm}^{-1}$. The

experimental data are taken from [39]. The self-consistent occupation probabilities for nuclear matter are in good agreement with experimental data.

5 Conclusion

In this paper the nucleon properties in the nuclear medium have been studied using a self-consistent self-energy. The effects of hole-hole contributions and a self-consistent treatment within the framework of the Green function approach are investigated. It is observed that the effects of hole-hole contributions in binding energies are not large, this represent a success for the BHF theory.

Müther and his collaborators [31] and Baldo and Fiasconaro [33] shown, that the parabolic approximation for the single particle potential $U(k)$ in the self-consistent Brueckner scheme introduces an uncertainty of 1-2 MeV near the saturation density, and therefore it cannot be used in accurate calculations. The full momentum dependence has to be retained, which prevents the use of a constant effective mass approximation. In this paper, we have explained that at high densities the parabolic approximation is valid.

The spectral functions are calculated from the momentum and energy dependent self-consistent self-energy by solving the Dyson equation. We found that the nuclear matter self-consistent occupation probabilities are in good agreement with the experimental measurements.

Acknowledgements

One of us (Kh. Gad) would like to thank Professor H. Müther for useful discussions, guidance and using his computer code.

References

- [1] B.D. Day, Rev. Mod. Phys. **39** (1967) 719.
- [2] D.W.L. Sprung, Adv. Nucl. Phys., ed. M. Branger and E. Vogt (plenum press, New York 1972) 5, (1972) 225.
- [3] M. Hjorth-Jensen, T.T. Kuo, and E. Osnes, Phys. Rep. **261** (1999) 125.
- [4] Y. Dewulf, W.H. Dickhoff, D. Van Neck, E.R. Stoddard, and M. Waroquier, Phys. Rev. Lett. **90** (2003) 152501.

- [5] F. Frömel, H. Lenske, and U. Mosel, Nucl. Phys. **A723** (2003) 544.
- [6] M. Baldo and L. Lo Monaco, Phys. Lett. **B525** (2002) 261.
- [7] M. Baldo, *Nuclear Methods and the Nuclear Equation of State*, Int. Rev. of Nucl. Physics, Vol. 9 (World-Scientific Publ. Comp., Singapore 1999).
- [8] H. Müther and A. Polls, Prog. Part. Nucl. Phys. **45** (2000) 243.
- [9] K. Brueckner, R.J. Eden, and N.C. Francis, Phys. Rev. **100** (1955) 891.
- [10] H.A. Bethe, Ann. Rev. Nucl. Sci. **21** (1971) 933.
- [11] M.I. Haftel and F. Tabakin, Nucl. Phys. **A158** (1970) 1.
- [12] J.P. Jeukenne, A. Lejeune, and C. Mahaux, Phys. Rep. **25** (1976) 83.
- [13] A. Ramos, W.H. Dickhoff, and A. Polls, Phys. Rev. **C43** (1991) 2239.
- [14] A. Ramos, W.H. Dickhoff, and A. Polls, Phys. Lett. **B219** (1989) 15.
- [15] A. Ramos, A. Polls, and W.H. Dickhoff, Nucl. Phys. **A503** (1989) 1.
- [16] Y. Dewulf, Ph.D. Thesis, University of Gent (2000).
- [17] W.H. Dickhoff and H. Müther, Rep. Prog. Phys. **11** (1992) 1947.
- [18] B.E. Vonderfech, W.H. Dickhoff, A. Polls, and A. Ramos, Nucl. Phys. **A555** (1993) 1.
- [19] Kh. Gad and H. Müther, Phys. Rev. **C66** (2002) 044301.
- [20] L.P. Kadanoff and G. Baym, *Quantum Statistical Mechanics* (Brnjamin, New York, 1962).
- [21] W.D. Kraeft, D. Kremp, W. Ebeling, and G. Röpke, *Quantum Statistics of Charged Particle Systems* (Akademie-Verlag, Berlin, 1986).
- [22] T. Frick and H. Müther, nucl-th/0306009.
- [23] H.S. Köhler, Phys. Rev. **C46** (1992) 1687.
- [24] H.S. Köhler and R. Malfiet, Phys. Rev. **C48** (1993) 1034.
- [25] C. Mahaux and R. Sartor, Adv. Nucl. Phys. **20** (1991) 1.
- [26] W.H. Dickhoff and H. Müther, Rep. Prog. Phys. **11** (1992) 1947.
- [27] A. Ramos, Ph.D. Thesis, Barcelona University (1988).
- [28] R. Machleidt, F. Sammarruca, and Y. Song, Phys. Rev. **C53** (1996) R1483.
- [29] R. Machleidt, Adv. Nucl. Phys. **19** (1989) 189.
- [30] H.A. Bethe, B.H. Brandow, and A.G. Petschek, Phys. Rev. **129** (1963) 225.
- [31] T. Frick, Kh. Gad, H. Müther, and P. Czerski, Phys. Rev. **C65** (2002) 034321.

- [32] Kh. Gad, Ph.D. Thesis, South Valley University, Sohag, (2002).
- [33] M. Baldo and A. Fiasconaro, Phys. Lett. **B491** (2000) 240.
- [34] P. Grange, J. Cugnon, and A. Lejeune, Nucl. Phys. **A473** (1987) 365.
- [35] H.S. Lehmann, Nuovo Cimento **11** (1954) 342.
- [36] V.M. Galitski and A.B. Migdal, Sov. Phys. JETP **34** (1958) 96.
- [37] J.M. Luttinger, Phys. Rev. **121** (1961) 942.
- [38] O. Benhar, A. Fabrocini, and S. Fantoni, Nucl. Phys. **A505** (1989) 267;
O. Benhar, A. Fabrocini, and S. Fantoni, Nucl. Phys. **A550** (1992) 201.
- [39] C. Ciofi degli Atti, E. Pace, and G. Salme, Phys. Rev. **C43** (1991) 1153.

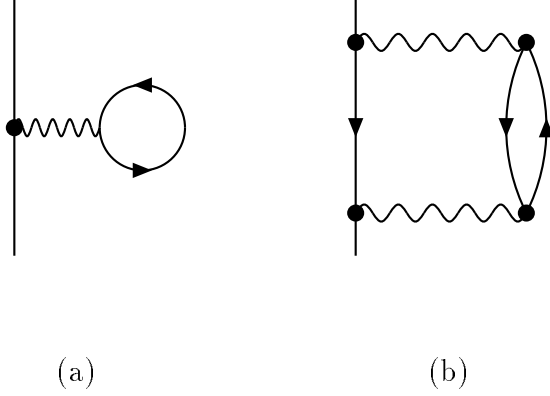


Figure 1. Diagrams contributing to the nucleon self-energy. The wavy lines indicate the Brueckner G-matrix. (a) The left diagram is the standard Brueckner approximation for the nucleon self-energy (4). (b) This diagram takes into account transitions to one-particle two-hole states. It contributes to both real and imaginary parts of the self-energy in the considered energy and momentum range.

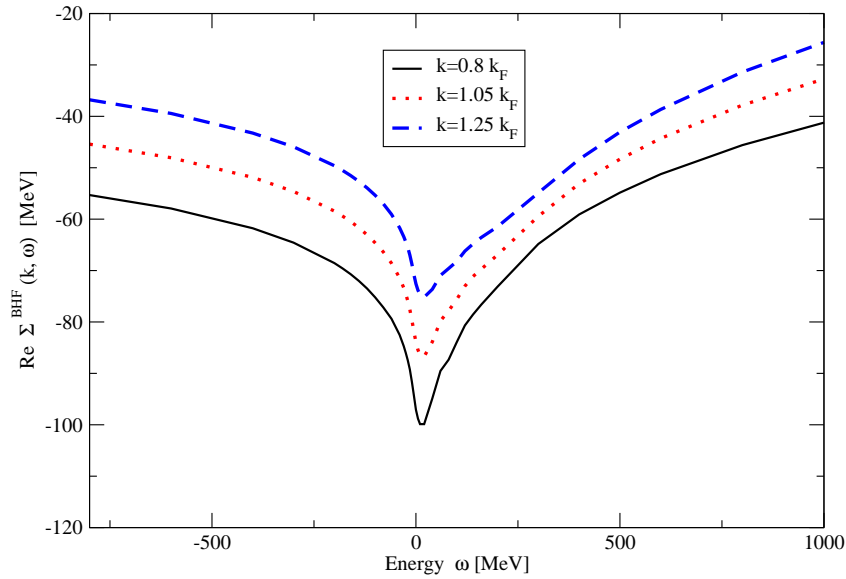


Figure 2. The real part of the BHF self-consistent self-energy as a function of the energy ω (see (4)) for symmetric nuclear matter with Fermi momentum $k_F = 1.36 \text{ fm}^{-1}$ evaluated for the CD-Bonn interaction, calculated for various momenta k .

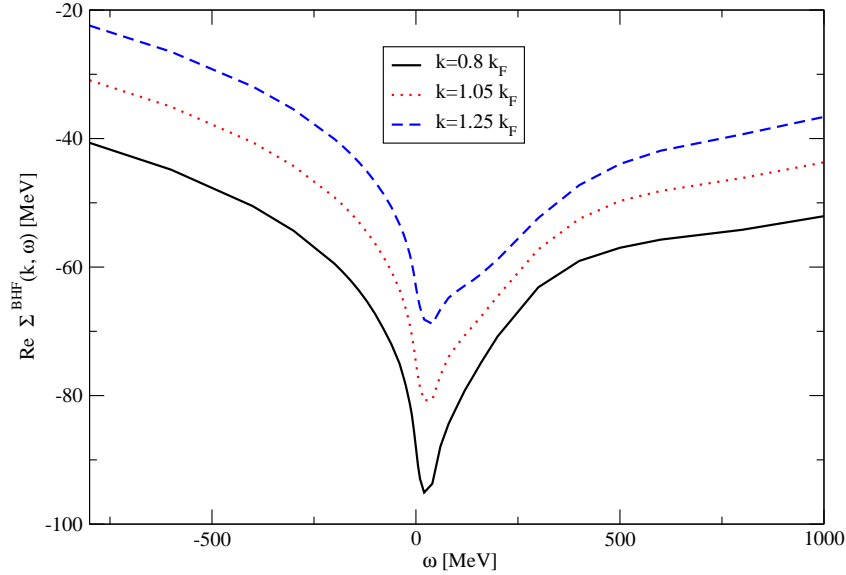


Figure 3. The real part of the BHF self-consistent self-energy as a function of the ω (see (4)) for nuclear matter with Fermi momentum $k_F = 1.36 \text{ fm}^{-1}$ evaluated for the Bonn C potential, for various momenta k .

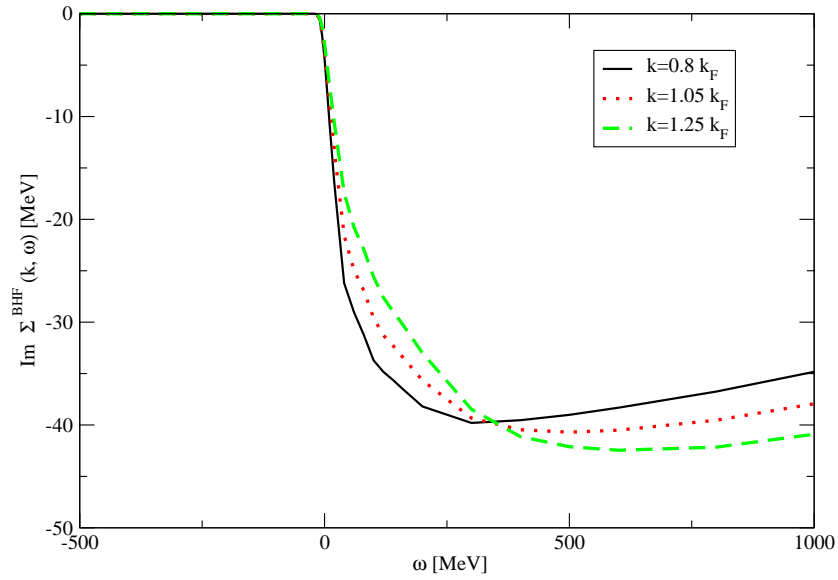


Figure 4. The imaginary part of the BHF self-consistent self-energy as a function of ω (see (4)) for nuclear matter with Fermi momentum $k_F = 1.36 \text{ fm}^{-1}$ calculated for the CD-Bonn interaction, calculated for various momenta k .

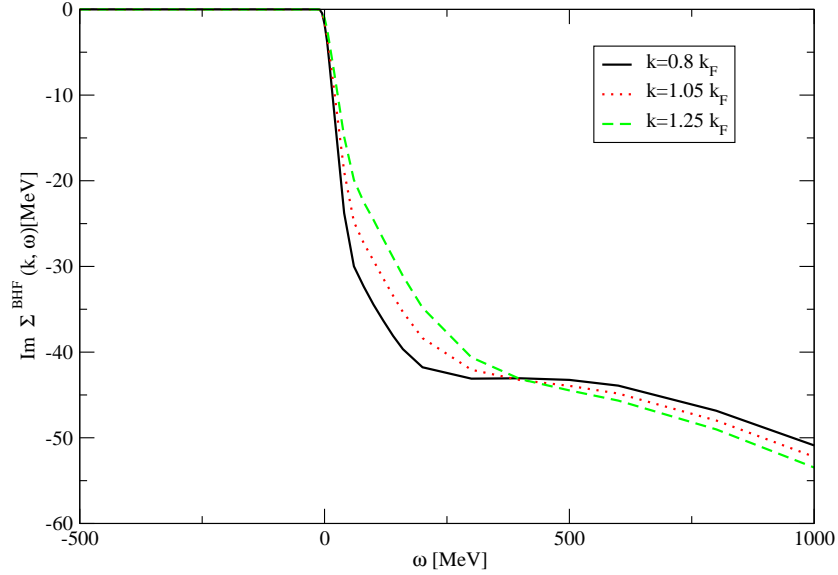


Figure 5. The imaginary part of the BHF self-consistent self-energy for nuclear matter with Fermi momentum $k_F = 1.36 \text{ fm}^{-1}$ calculated for the Bonn C interaction, calculated for various momenta k .

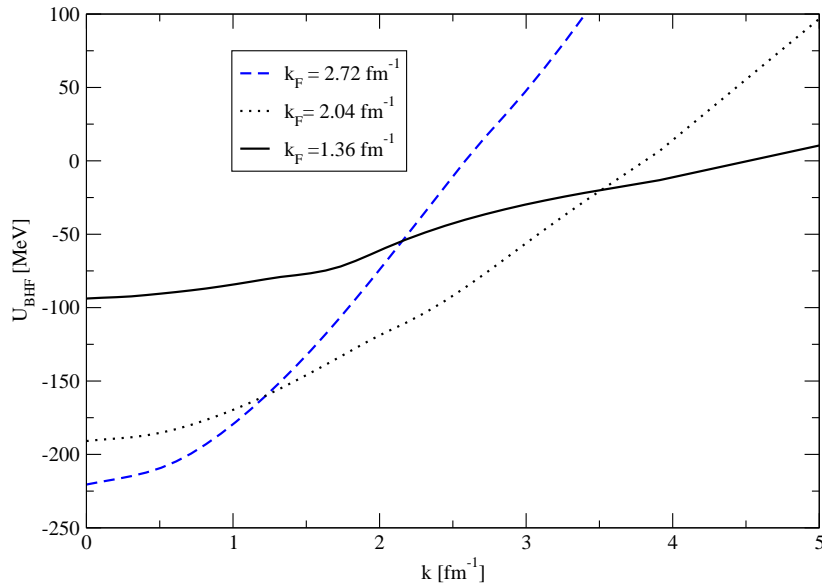


Figure 6. The single-particle self-consistent potentials U_{BHF} (see (12)) as a function of momentum. Results are displayed at $k_F = 1.36 \text{ fm}^{-1}$, $k_F = 2.04 \text{ fm}^{-1}$ and $k_F = 2.72 \text{ fm}^{-1}$ using the CD-Bonn potential.

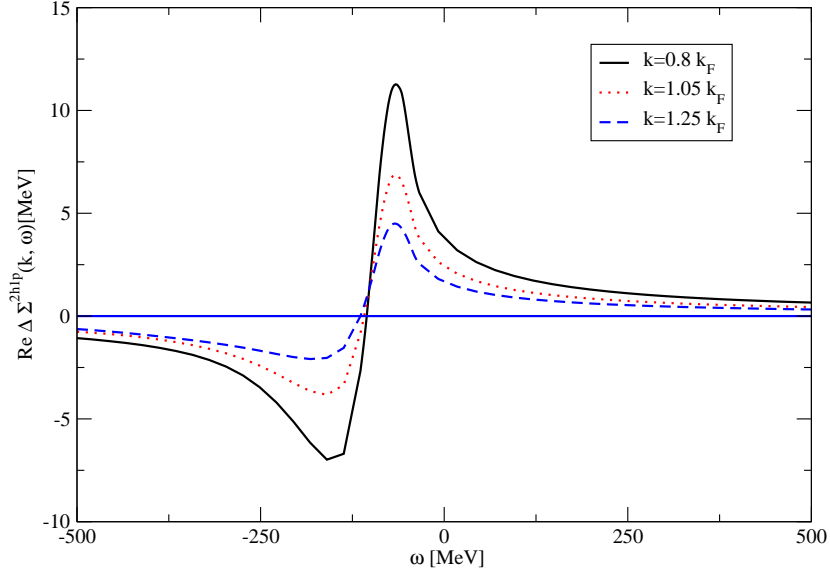


Figure 7. The real part of the 2h1p contribution to the self-consistent self-energy as a function of ω (see (13)) evaluated for the CD-Bonn potential assuming $k_F = 1.36 \text{ fm}^{-1}$ for various momenta k .

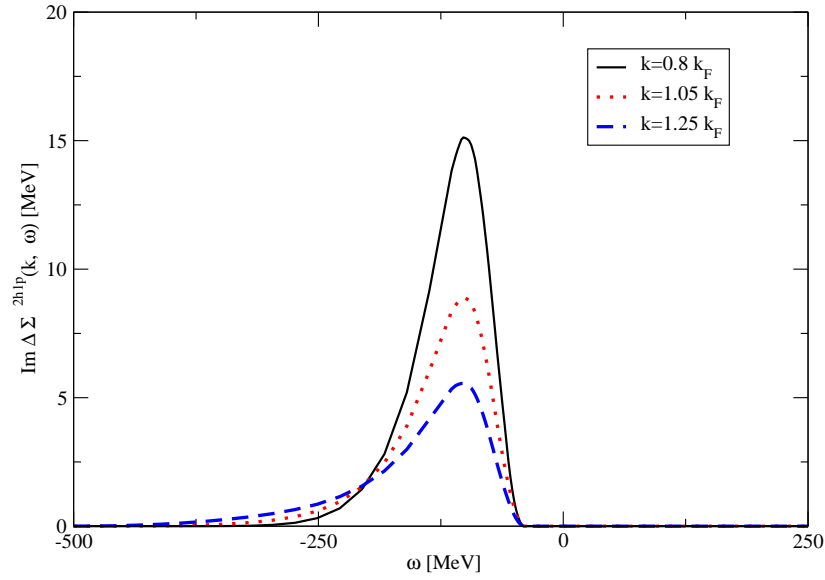


Figure 8. The imaginary part of the 2h1p contribution to the self-consistent self-energy as a function of ω (see (13)) evaluated for the CD-Bonn potential assuming $k_F = 1.36 \text{ fm}^{-1}$ for various momenta k .

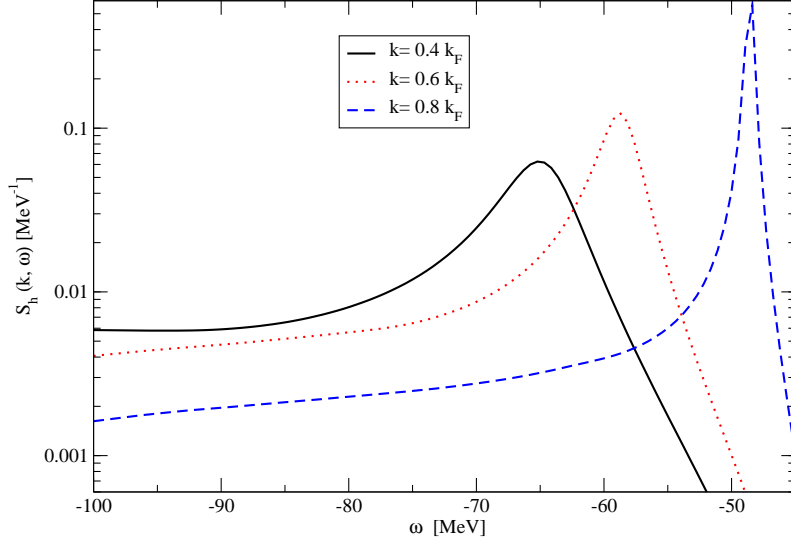


Figure 9. Hole self-consistent spectral functions $S_h(k, \omega)$ as a function of ω for three different momenta in nuclear matter at $k_F = 1.36 \text{ fm}^{-1}$ assuming the CD-Bonn potential. Note the narrowing of the peak in the spectral function when k gets closer to k_F .

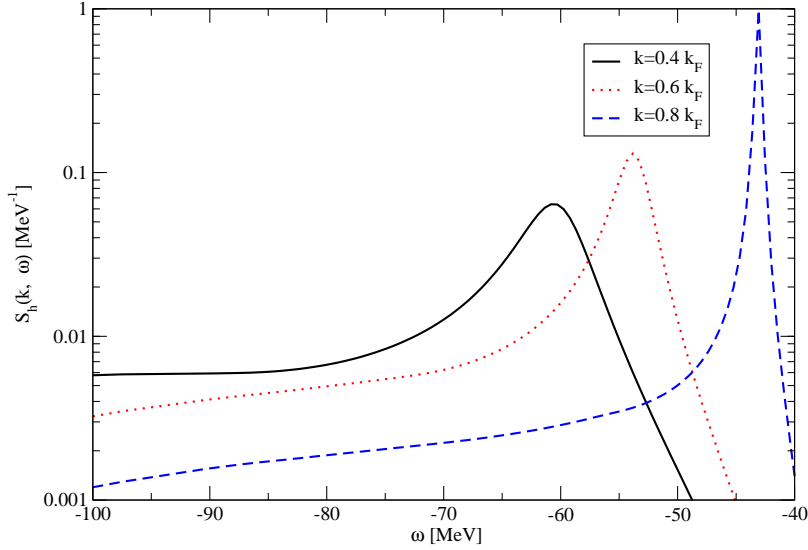


Figure 10. Hole self-consistent spectral functions for three different momenta below k_F in nuclear matter at $k_F = 1.36 \text{ fm}^{-1}$ using the Bonn C potential.

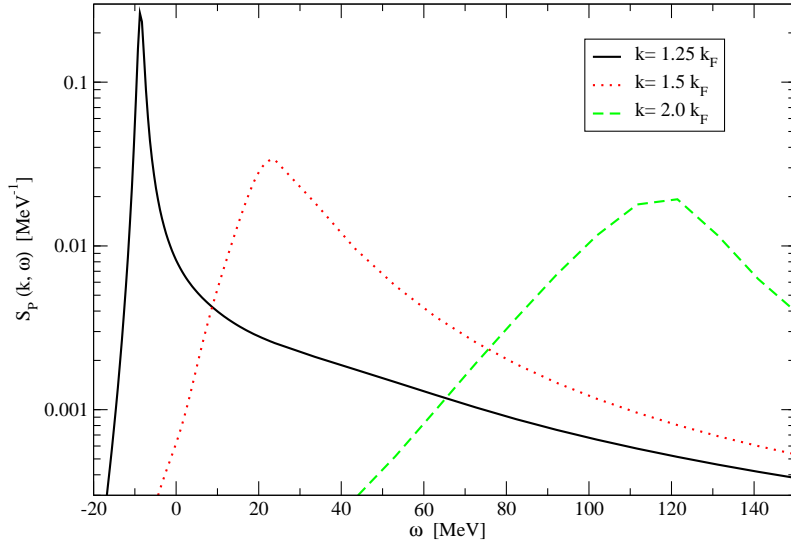


Figure 11. Particle self-consistent spectral functions $S_p(k, \omega)$ as a function of energy for various momenta showing a broadening quasi particle peak with increasing momentum. The data have been obtained for nuclear matter using the CD-Bonn potential with a Fermi momentum $k_F = 1.36 \text{ fm}^{-1}$ and using gab choice.

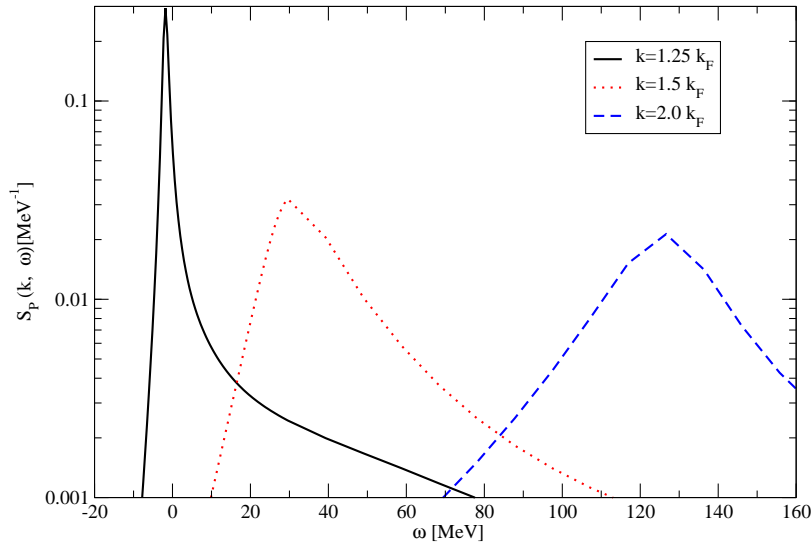


Figure 12. Particle self-consistent spectral functions for $k = 1.25, 1.5,$ and $2.0 k_F$. The results have been obtained for nuclear matter with a Fermi momentum $k_F = 1.36 \text{ fm}^{-1}$ and using gab choice, assuming the Bonn C potential.

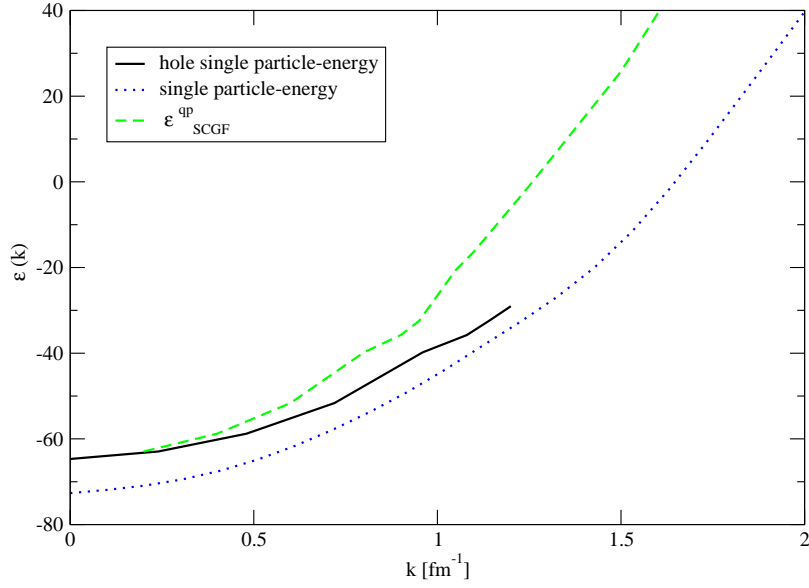


Figure 13. The single-particle energy $\varepsilon(k)$ (see (10) and (11)) as a function of the momentum at $k_F=1.2 \text{ fm}^{-1}$ using the CD-Bonn potential. For the single particle energy for BHF using continuous choice, single particle energy below k_F for SCGF and quasi particle energy (20).

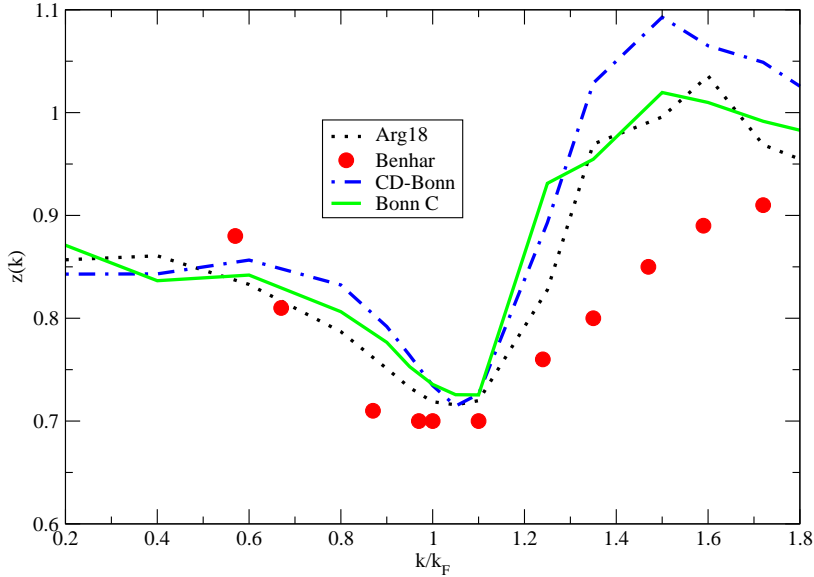


Figure 14. Quasi particle strength in nuclear matter at $k_F=1.36 \text{ fm}^{-1}$ (see (21)) using various models for the NN interaction. For comparison, results from the full many-body calculation of Benhar *et al.* [38] (dots) at $k_F=1.33 \text{ fm}^{-1}$ are also shown.

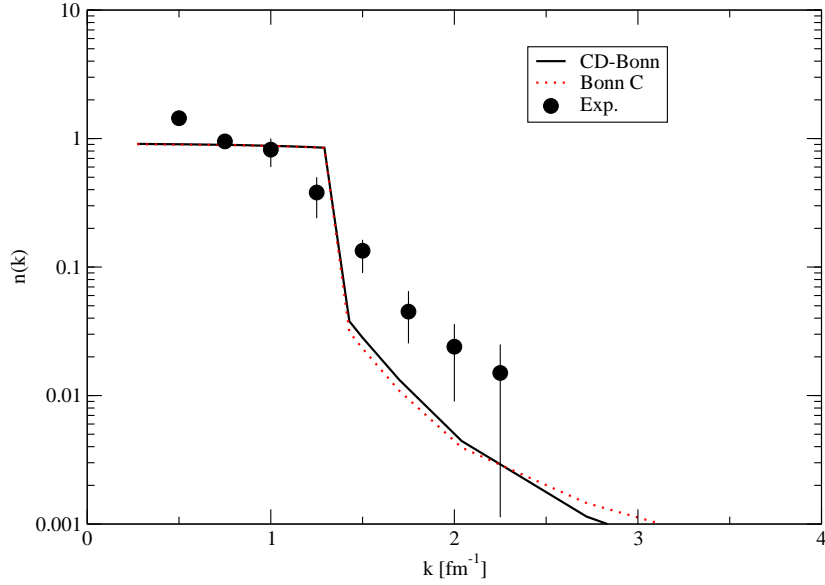


Figure 15. Momentum distribution in nuclear matter calculated from the spectral function. Results are given for the CD-Bonn and Bonn C potential at $k_F = 1.36 \text{ fm}^{-1}$. The experimental data are from [39].

Table 1

Energy per nucleon for nuclear matter considering three different densities, $k_F = 1.20, 1.36$ and 1.60 fm^{-1} , assuming the CD-Bonn potential. Results are displayed for HF, BHF with a continuous choice and using the exact Pauli operator [31], and the BHF+2h1p using conventional choice where the self-energy is calculated self-consistently. All energies are given in MeV per nucleon.

	$k_F \text{ [fm}^{-1}\text{]}$	HF	BHF, exact [31]	(BHF+2h1p)
	1.20	2.88	-15.39	-15.34
CD-Bonn	1.36	4.61	-18.83	-18.99
	1.60	10.31	-22.86	-22.78